RESEARCH ARTICLE

Purification of mitochondria from skeletal muscle tissue for transcriptomic analyses reveals localisation of nuclear-encoded non-coding RNAs

Authors:

Jessica Silver[1] and Adam J. Trewin[1] (co-first authors), Stella Loke[2], Larry Croft[2], Mark Ziemann[3], Hayley Dillon[1,4], Søren Nielsen[5], Séverine Lamon[1], Glenn. D. Wadley[1]

Affiliations:

[1]Institute for Physical Activity and Nutrition, School of Exercise and Nutrition Sciences, Deakin University, Geelong, Victoria, Australia.

[2]Genomics Centre, School of Life and Environmental Sciences, Deakin University, Geelong, Victoria, Australia.

[3]School of Life and Environmental Sciences, Deakin University, Geelong, Victoria, Australia.

[4]Human Integrated Physiology and Sports Cardiology Laboratory, Baker Heart and Diabetes Institute, Melbourne, Australia.

[5]The Centre of Inflammation and Metabolism and the Centre for Physical Activity Research, Rigshospitalet, University of Copenhagen, Copenhagen, Denmark.

Corresponding author:

Prof. Glenn Wadley

Deakin University

Institute for Physical Activity and Nutrition,

School of Exercise and Nutrition Sciences,

Australia

3125

Email: glenn.wadley@deakin.edu.au

ABSTRACT

Mitochondria are central to cellular function, particularly in metabolically active tissues such as skeletal muscle. Non-coding RNAs (ncRNAs) typically localise within the nucleus and cytosol but may also translocate to subcellular compartments such as mitochondria. We aimed to investigate the nuclear-encoded ncRNAs that localise within the mitochondria of skeletal muscle cells and tissue. Intact mitochondria were isolated via immunoprecipitation and an enzymatic digestion approach was optimised to remove transcripts located exterior to mitochondria, making it amenable for high-throughput transcriptomic sequencing. Small-RNA sequencing libraries were successfully constructed from as little as 1.8ng mitochondrial RNA input. Small-RNA and whole transcriptome sequencing of mitochondria reveals the enrichment of over 200 miRNAs and 200 lncRNAs that have not previously been observed within skeletal muscle mitochondria. In summary, we describe a novel, powerful sequencing approach applicable to animal and human tissues and cells that reveals the unexpected diversity of nuclear-encoded ncRNA transcripts localised within skeletal muscle mitochondria.

152 words

INTRODUCTION

Mitochondria are subcellular organelles essential for numerous cellular processes including energy metabolism, signalling, ion and redox homeostasis as well as regulation of apoptosis (Spinelli and Haigis, 2018). Mitochondria are comprised of proteins encoded by both the nuclear and mitochondrial genomes, but nuclear-encoded RNAs are not usually localised within mitochondria. A small number of specific RNAs, such as microRNAs (miRNAs) (Barrey et al., 2011, Sripada et al., 2012, Das et al., 2012) and long non-coding RNAs (lncRNAs) (Noh et al., 2016) can however be imported into mitochondria (Silver et al., 2018) via the polynucleotide phosphorylase (Wang et al., 2010) and other putative transport mechanisms (reviewed in Silver et al., 2018). Because ncRNAs have the ability to regulate various transcriptional and translational processes relating to mitochondrial function, it is of interest to determine which of these may localise within mitochondria in order to understand the nature of their potential regulatory actions.

Investigations into mitochondria-localised nuclear-encoded ncRNAs have been constrained, first, by the technical challenges of obtaining pure mitochondrial preparations free of confounding RNAs peripheral to isolated mitochondria and, second, by the significantly lower RNA yields from subcellular fractions when compared to whole tissue homogenates. Early studies providing evidence for the localisation of ncRNAs within mitochondria stem from micro-array analysis and are routinely validated by single qPCR assays or *in situ* hybridisation (Barrey et al., 2011, Sripada et al., 2012, Das et al., 2012). However, the overall population of ncRNAs that localise within mitochondria and their regulatory actions remain unknown.

Skeletal muscle constitutes ~40% of human body mass and plays a central role in whole body metabolism (Zurlo et al., 1990). To meet these dynamic bioenergetic demands, skeletal muscle is densely populated with mitochondria (Russell et al., 2014). Thus, gaining a greater understanding of the RNA profile within muscle mitochondria may yield important insights into the cellular biology and aetiology of diverse metabolic diseases characterised by mitochondrial dysfunction, such as diabetes mellitus and chronic myopathies (Silver et al., 2018). Here, we report a method for isolating and optimising the enzymatic purification of mitochondria from rodent muscle cells or tissues. We provide direct evidence for the purity of this mitochondrial fraction, making it amenable for downstream high-throughput analyses. Finally, we describe a method suitable for small-RNA and whole transcriptome sequencing of mitochondria isolated from skeletal muscle cell and tissue samples from animals and humans, and report the enrichment of numerous nuclear-encoded RNAs that have not previously been observed within skeletal muscle mitochondria.

RESULTS

Protease purification of isolated mitochondria

We first isolated mitochondria from cultured L6 rat myoblasts using an antibody against an outer mitochondrial membrane protein (TOMM22) conjugated to magnetic beads allowing for precipitation of intact isolated mitochondria (Figure 1). Immunoblot of the post-precipitation mitochondrial fraction revealed that a small amount of α-tubulin and Lamin B1 (used as protein markers of the cytosol and nucleus, respectively) were present in the isolated mitochondria fraction (Figure 2, lane 1). The isolated mitochondrial fraction was then incubated with a serine protease (proteinase-K) to digest proteins not located within the mitochondrial intermembrane space (IMS) or matrix compartments. This led to depletion of α-tubulin and Lamin B1, in addition to a marker of the outer mitochondrial membrane (TOMM20). Intermembrane space (cytochrome-*c*) and matrix protein markers (citrate synthase) were protected from digestion (Figure 2, lane 2). All proteins probed were susceptible to proteinase-K when mitochondrial membranes were dissolved in the presence of detergent (triton-X, Figure 2, lane 3). Together, this demonstrates that mitochondrial isolation by TOMM22-immunoprecipitation followed by enzymatic treatment yields a purified, intact mitochondrial fraction suitable for downstream protein analyses. Based on this, we hypothesised that an analogous approach could be used with a ribonuclease to remove RNA located outside of isolated mitochondria.

Ribonuclease purification of isolated mitochondria

Next, mitochondria isolated from L6 myoblasts were exposed to a range of concentrations of RNase-A (Figure 3), an endonuclease that cleaves phosphodiester bonds after pyrimidine residues in the RNA molecule (Witzel, 1963). RNase-A-treated isolated mitochondria were assessed by RT-qPCR for abundance of mtDNA-encoded mRNA (*Mt-co3*) that localises exclusively within the mitochondrial matrix compartment, and a nuclear-encoded mRNA (*Cox4i1*) that localises outside mitochondria. We found that *Mt-co3* was protected from degradation at RNase concentrations up to at least 100 µg/mL, whereas partial *Cox4i1* degradation occurred at 10 µg/mL and was mostly degraded at 100 µg/mL (Figure 3). In the presence of detergent, 1 µg/mL RNase-A was sufficient to digest all *Cox4i1* and *Mt-co3*, as well as an exogenous mRNA spike-in control (Figure 3). This suggests that a certain proportion of cytosolic *Cox4i1* is protected from digestion at lower RNase-A concentrations, potentially as a result of being bound to ribosomes at the outer mitochondrial membrane (Gold et al., 2017). Taken together, these data suggest that TOMM22-IP mitochondrial isolation followed by RNase-A treatment is suitable for downstream mitochondrial RNA analyses provided the RNase-A concentration is optimised to remove transcripts not located within the mitochondrial membranes.

Concurrent investigations have confirmed that RNase-A concentrations exceeding 100 µg/mL are suitable for use in human tissue analysis. This approach successfully removes non-mitochondrial

RNA in isolated mitochondria from human skeletal muscle biopsy samples, and is suitable for the detection of mitochondria-localised miRNAs (Supplementary Table 1).

Small RNA sequencing on purified isolated mitochondria from myoblast reveals mitochondria localised miRNAs

Having established optimal RNase-A conditions to obtain purified mitochondria, we next optimized a protocol to perform transcriptomic analysis of the small RNAs (sRNA) contained within this fraction. We first prepared sRNA libraries from 120 ng and 60 ng mitochondrial RNA with 0.5X adapter dilutions (NEBNext 3´ and 5' SR Adaptors, and RT primer for Ilumina), in line with the standard manufacturer protocol (NEBNext Multiplex Small RNA Library Prep Set (New England Biolabs). The standard protocol produced large amounts of adapter-dimer and was not sufficient to ligate adapters to the target miRNAs within the sample (Figure 4 A, B). We next decreased the amount of the 3' and 5' adapters to investigate if a lower molar ratio improved miRNA ligation efficiency. Both the modified-0.3X (Figure 4 C) and modified-0.1X (data not shown) approaches produced quantifiable amounts of the target miRNA library when prepared from 60 ng mitochondrial RNA, although the total cDNA yield was approximately 7-fold higher from the modified-0.3X when compared to modified-0.1X protocol. Both modified approaches did decrease, but not prevent, adapter-dimer formation.

While 60 ng mitochondrial RNA is below the recommended library RNA input (>100 ng, NEBiolabs, Inc.), mitochondrial RNA yield from cell and tissue samples is often considerably below this threshold. Thus, it was necessary to investigate if the modified-0.3X and modified-0.1X approach could similarly produce the target miRNA library when prepared from much lower amounts of mitochondrial RNA. The modified-0.3X (Figure 4 C, D) and modified-0.1X (data not shown) approaches both produced the target library when prepared from >1.8 ng (range 1.8-60 ng) mitochondria RNA. Total cDNA yields were, on average, 4.3-fold higher ($p<0.05$) when using the modified-0.3X protocol compared to the modified-0.1X. The presence of adapter-dimer dominated each library, regardless of the mitochondrial RNA input amount used. To combat this, all uniquely indexed libraries were combined in an equimolar pool and run across two lanes of a TBE polyacrylamide gel. The gel fragment corresponding to the miRNA region was manually excised, extracted from the gel and then sequenced. There were no differences in total RNA-seq reads ($p=0.79$) and total mapped miRNA reads ($p=0.19$) between the modified-0.3X and modified-0.1X protocols (Figure 5). Over 200 miRNAs were detected across all but the lowest (1.8ng, modified-0.1X) mitochondrial RNA inputs (Figure 6). The number of miRNAs detected appeared to plateau when libraries were prepared from 15-60ng mitochondrial RNA (Figure 6B) and suggests that RNA inputs of at least 15ng are sufficient to detect most miRNAs within a sample. Ultimately, either modified approach is suitable for the production of miRNA libraries. However, the significantly higher library

yields make the modified-0.3X approach amenable to library pooling, gel excision, and subsequent sequencing.

We next investigated the relative abundance of miRNAs sequenced from serial dilutions of mitochondrial RNA input (1.8-30 ng), when compared to the highest mitochondria RNA input (60 ng). Most miRNAs detected were common between libraries prepared from 60 ng mitochondria RNA and the lower mitochondria RNA inputs (Figure 7A-C). Further to this, the relative abundance of miRNAs was comparable between libraries prepared from the two highest RNA inputs (60 vs 30 ng; Figure 7F). A small number of miRNA species were over- (8 miRNAs) and under-represented (5 miRNAs) within libraries prepared from the highest RNA input (60 ng) when compared to lowest RNA input (1.8 ng; Figure 7D). MiRNAs detected in the highest, but not lowest, RNA input displayed low expression levels within the 60 ng sample, and together constituted a small proportion (1069 rpm) of total reads. Interestingly, the skeletal muscle-enriched miR-1, miR-133a, miR-133b and miR-16 and miR-486, predicted to have roles in the regulation of mitochondrial function (Nielsen et al., 2010, Russell et al., 2013), were detected at higher mitochondria RNA inputs (60 and 30 ng), but not lower inputs (1.8-15 ng; Figure 7). In contrast, the let-7 family as well as the skeletal muscle-enriched miR-206 were highly abundant in all samples, and together constituted 63±8% of all mapped miRNA reads. Importantly, the relative distribution of miRNAs within each sample provides adequate representation across serial dilutions of mitochondrial RNA, making it possible to accurately investigate differential miRNA expression across unique cell and tissue samples with variable mitochondrial RNA yields.

Together, these data suggest that stringent optimization is required when preparing sRNA libraries from low amounts of RNA from purified mitochondria. To minimize adapter-dimer presence in sRNA libraries, gel excision and purification of the target miRNA fraction is recommended. Importantly, our data demonstrate that RNA-seq results were comparable across serial dilutions of mitochondrial RNA input, suggesting that low mitochondria RNA input does not limit the number nor the relative distribution of miRNA species that can be detected.

<u>Total RNA-sequencing of isolated mitochondria from rat skeletal muscle tissue reveals selective enrichment of nuclear-encoded non-coding RNAs</u>

To gain further insight into the RNA landscape within mammalian muscle mitochondria, we then applied the mitochondrial isolation and purification strategies described above to the gastrocnemius tissue of 9-week old rats. Whole-transcriptome RNA sequencing revealed that these mitochondria had a high degree of purity as indicated by the following observations. Firstly, there was a low relative proportion of nuclear-encoded mRNAs unrelated to mitochondria, such as genes associated with muscle sarcomere function i.e. myosin light (e.g. *Myl1*) and heavy (e.g. *Myh4* and *Myh7*) isoforms, α-actin (*Acta1*) and troponins (e.g. *Tnnc2*, *Tnnt3*; Figure 8A). Secondly, the mitochondrial fraction also

contained a low relative abundance of nuclear-encoded OXPHOS genes (including *Cox4i1)*, as expected (Figure 8B). Thirdly, there was similar abundance of all mtDNA-encoded OXPHOS transcripts including *Mt-co3* between the whole tissue and mitochondrial fractions (Figure 8C). This serves as an important internal control because mtDNA transcripts should be present in both isolated mitochondria and whole tissue in similar proportions. Based on these assumptions, we observed that non-coding RNAs were enriched in the mitochondrial fraction relative to the respective whole tissue, including 222 long non-coding RNAs and 102 pseudogenes, ((FDR $\leq$0.05, log2FC $\geq$1, Figure 8D and Supplementary Figure 1). The vast majority of these non-coding RNA transcripts are of unknown function. Additionally, there were 49 transcripts that encode miRNA genes (i.e. primary- or pre-miR transcripts) that were also detected in the mitochondrial fraction (Figure 8D and Supplementary Figure 1).

DISCUSSION

Studies of subcellular fractions using high-throughput analyses requires careful consideration of purification strategies to avoid confounding effects of contaminants. Here we report an optimised method for purification of isolated mitochondria for downstream transcriptomic analysis. Revealing the utility of this approach, we confirmed that miRNAs can be reliably detected in the mitochondria of L6 myoblasts even when libraries are prepared from RNA inputs well below the thresholds often recommended by manufacturers. Following this, we report, for the first time, the selective enrichment of various nuclear-encoded non-coding RNAs within rat skeletal muscle mitochondria.

Incubation of isolated mitochondria with RNase-A can be used to degrade contaminating, non-mitochondrial RNA to ensure that only RNA species contained within the mitochondria membranes are used in downstream analyses. This is important when investigating transcripts that do not localise in one subcellular compartment, but instead may be actively transported between the mitochondria and cytosol in response to various physiological stimuli. RNase-A protocols differ substantially between studies that have investigated mitochondrial RNA expression. In previous studies, RNase-A has been used at variable final concentrations (5-50 μg/mL) (Barrey et al., 2011, Mercer et al., 2011, Zhang et al., 2014, Bandiera et al., 2011) or has been omitted entirely (Das et al., 2012, Dasgupta et al., 2015, Lung et al., 2006, Sripada et al., 2012). Here, we demonstrate that RNase-A concentrations of at least 100 μg/mL are required to digest the majority of nuclear-encoded transcripts (such as *Cox4i1*) in rat myoblasts. Importantly, this approach is transferable between cell and tissue models and is shown to effectively degrade potentially contaminating, non-mitochondrial RNA in mitochondria isolated from human skeletal muscle tissue (Supplementary Table 1).

Investigations into the mitochondrial ncRNA population are often limited by technical challenges. For example, the inherently low mitochondrial RNA yields compared to total cellular RNA are well below the threshold required for commercially available small RNA library preparation protocols. This

challenge may be overcome by combining mitochondria RNA from biological samples into pools that represent a single 'intervention' or 'clinical' group, and the 'control' group (Jagannathan et al., 2015, Wang et al., 2017). While this effectively increases the amount of mitochondrial RNA available for sRNA library preparation, this approach introduces further limitations. First, the use of pooled samples requires a much larger sample size to achieve the same statistical power (Takele Assefa et al., 2020). Second, gene expression is highly variable between individuals; taking a pooled sample approach may mask potential individual variability in miRNA expression (Takele Assefa et al., 2020, Rajkumar et al., 2015). Our findings illustrate that small RNA libraries can be prepared from individual biological samples without the need to pool multiple samples, thereby increasing the statistical power available, especially for human studies with limited sample material and high participant burden.

A modified small RNA library preparation protocol increased ligation efficiency of the 3' and 5' adapters to miRNAs within mitochondrial samples. However, this modified approach was not able to prevent adapter-dimer formation entirely. As the adapter-dimer product is approximately 20 bp smaller than adapter-ligated miRNAs and preferentially binds to the flow cell during RNA-Seq, gel extraction of the target miRNA region is essential to maximise read counts that map to miRNAs rather than adapter-dimer (Shore et al., 2016). When used together, the modified-0.3X protocol plus gel extraction were successful in detecting over 200 miRNAs from L6 mitochondria RNA inputs as low as 1.8 ng. Importantly, the relative distribution of miRNAs within each sample was reasonably consistent as RNA input decreased. However, some miRNA species tended to be over-represented at the lowest mitochondria RNA inputs. This may be because there were less miRNA species detected in the library prepared from 1.8 ng (207 miRNAs) when compared to 60ng mitochondria RNA (266 miRNAs). Overall, there appears to be minimal bias towards over- or under-representing specific miRNA species at low RNA inputs.

Of note, the skeletal muscle-enriched miR-1, miR-133a and miR-133b were detected at high (30 and 60 ng) but not low (1.8-15 ng) mitochondrial RNA inputs. MiR-1 and miR-133a have previously been observed in mitochondria isolated from human skeletal and rodent cardiac muscle cells *in vitro* (Barrey et al., 2011, Jagannathan et al., 2015, Zhang et al., 2014). MiR-1 enhances the transcription of the mitochondrial-encoded mt*Cox1*, mt*Nd1* and mt*Cytb*, among others (Zhang et al., 2014), while miR-133a inhibits the transcription of nuclear-encoded *PGC-1* isoforms and *Tfam* (Nie et al., 2016), both of which are upstream regulators of mitochondrial biogenesis. The use of proliferating L6 myocytes in this study, compared with primary human myocytes (Barrey et al., 2011) and rat neonatal cardiomyocytes (Zhang et al., 2014) used previously, may partially account for the differences in miRNA species detected. Although L6 cells have reportedly higher rates of aerobic metabolism when compared to C2C12 cells and primary human myocytes, cell culture models are more dependent upon anaerobic glycolysis (Abdelmoez et al., 2020). Thus, mitochondrial abundance and function in

various cell culture models may differ to those observed with *in vivo* models. This study was primarily designed to optimise the ncRNA-Seq library preparation protocol rather than investigate the physiological relevance of specific miRNAs. Future *in vivo* studies are now required to profile mitochondrial miRNAs and their roles in tissues that have high bioenergetic requirements such as skeletal and cardiac muscle.

Finally, the enrichment of non-coding RNAs, including lncRNAs and pseudogenes, within mitochondria relative to whole skeletal muscle tissue suggests that a previously underappreciated scale of RNA import and/or regulation may occur at the subcellular level. Only a relatively small fraction (~5-10%) of all identified lncRNAs have been functionally characterized (Gao et al., 2020). LncRNA can have important regulatory roles (Wadley et al., 2019), mediating cellular processes by modulating the expression of genes, stability of transcripts and/or function of proteins (Long et al., 2017), including those that directly determine mitochondrial function. Individual validation and functional characterisation of the lncRNAs identified in the present study is required to understand the precise mechanisms involved and potential functional implications. This may also open new avenues of investigation into how they are imported into the mitochondrial compartment, what are their putative binding target(s) and whether they modulate expression levels of mtDNA encoded genes and/or function of mitochondrial proteins. This will be key to understanding the potential effects on mitochondrial parameters such as oxidative phosphorylation, ROS production, mitochondrial biogenesis, dynamics or mitophagy.

In summary, we report a method for obtaining a highly pure fraction of mitochondria from skeletal muscle tissue and optimised approach for high throughput transcriptomic sequencing on this subcellular fraction. Importantly, we reveal the presence of non-coding RNAs within mitochondria that were not previously known to reside within this subcellular compartment. Given the increasing interest in non-coding RNA mediated regulation of cellular function in health and disease, future investigations are warranted to better understand the potential biological and physiological significance of the mitochondrial localisation of these non-coding RNAs.

MATERIALS AND METHODS

Cell culture

L6 rat myoblast cells were obtained from a commercial vendor (ATCC Cat# CRL-1458, RRID: CVCL_0385). Cells were cultured at 37□ with 5% CO_2 in a humidified incubator in media consisting of Dulbecco's Modified Eagle Medium (DMEM; Gibco #11995-065) supplemented with 10% v/v FBS (Gibco #A3161001), 100 U/ml penicillin and 100 μg/ml streptomycin (Gibco #15140-122). Cells were grown in 150 mm dishes to ~90% confluence then washed with sterile PBS and detached (Gibco

TrypLE Express #LTS12604021). Cells used for all experiments were ≤9 passages from stock and tested negative for mycoplasma contamination (Agilent MycoSensor QPCR Assay Kit, 302107).

Myoblast mitochondrial isolation

Mitochondria were isolated from L6 myoblasts via immunoprecipitation (Miltenyi Biotek #130-096-946). Approximately $5x10^6$ cells (suspended in a small volume of PBS after detachment) were transferred to 1 mL ice-cold lysis buffer, then mechanically homogenised with 20 passes in a 7 mL glass dounce homogeniser (Wheaton) on ice. Wash buffer (9 mL) was added to the lysate and transferred to a falcon tube. Anti-TOMM22 antibody conjugated magnetic beads (50 µL) were added to the 10 mL lysate and incubated with gentle inversion for 1 hour at 4□. Lysate was passed through a pre-separation filter then flowed through a column mounted on a magnetic rack. Captured mitochondria were washed 3 times before being removed from the magnetic rack for elution. Mitochondria were pelleted via centrifugation at 13,000 x g for 2 minutes at 4□. Supernatant was then removed and the mitochondrial pellet resuspended in storage buffer to be used for subsequent purification.

Enzymatic purification of myoblast mitochondria

Protease treatment: To remove proteins not localised within intact mitochondria, aliquots of isolated mitochondria (1 µg total protein each) were incubated in a 50 µL reaction with or without triton-x (1% v/v) and with or without proteinase K (Qiagen #19131, final concentration 20 µg/mL) for 15 minutes at room temperature. Phenylmethylsulfonyl fluoride (20 mM) was added to inhibit proteinase-K. Samples were then stored at -20□ until immunoblot analysis.

RNase treatment: To remove RNA not localised within intact mitochondria, in a 50 µL reaction, aliquots of isolated mitochondria (1 µg total protein each) first had 100 ng mRNA spike-in control added (StemMACS eGFP mRNA #130-101-114, Miltenyi Biotec), and were then incubated with or without triton-x (1% v/v) and with or without RNase-A (Qiagen #19101, final concentration range 1-1000 µg/mL) and incubated on ice for 30 minutes. Trizol reagent was then added to simultaneously inactivate RNase activity and preserve RNA. Samples were then stored in Trizol at -20□ until RNA isolation.

Immunoblot analysis

Mitochondrial samples from proteinase-K treatment were thawed and resuspended in RIPA buffer (Millipore #20-188) containing protease inhibitors (Sigma #P8340). Protein concentration was determined by BCA assay (Pierce #23225). Samples were mixed with reducing loading buffer (4x Laemmli sample buffer with 10% 2-mercaptoethanol). Equal volumes of mitochondrial samples (0.2 µg total protein) were loaded into a 4-15% gel (Bio-Rad #5678085) in addition to whole cell lysate (12 µg) and molecular weight marker (Bio-Rad #161-0373), which were then separated by

electrophoresis at 40 V for 30 min then 120 V for 60 min. The stain-free gel was UV-activated for 1 minute and imaged for total protein (BioRad Chemi Doc XR+, Hercules, CA, USA) with ImageLab software (BioRad Image Lab v6). Protein was then transferred (Turbo Transfer system, Bio-Rad) to a methanol soaked polyvinylidene difluoride (PVDF) membrane (Millipore Immobilon FL 0.45 µm #IPFL00010). The membrane was then PBS washed, dried for 1 hour, re-wetted with methanol, washed with PBS then blocked for 1 hour (Li-Cor Intercept PBS blocking buffer). The membrane was then incubated with primary antibody in blocking buffer + 0.2% v/v Tween-20 overnight at 4°C. Primary antibodies used were: anti-TOMM20 (Abcam #ab186735; 1:1000), anti-Cytochrome-c (Abcam #ab133504; 1:1000), anti-Citrate Synthase (Cell Signaling Technology #14309; 1:1000), anti-α-Tubulin (Cell Signaling Technology #3873; 1:1000), and anti-Lamin B1 (Cell Signaling Technology #12586; 1:1000). Membranes were then washed with PBST and incubated with secondary antibodies (Cell Signaling Technology) anti□rabbit or anti□mouse IgG Dylight® 680 nm (Cell Signaling Technology #5366S, #5470S) or 800 nm (Cell Signaling Technology #5151S or #5257S) at 1:10,000 in blocking buffer containing 0.2% Tween-20 and 0.01% SDS for 1 hour at room temperature. Fluorescent signal was then digitally acquired (Licor Odyssey® Infrared Imaging System, Lincoln, NE, USA).

RNA isolation and quality control

Myoblast mitochondria samples stored in Trizol were thawed on ice and centrifuged at 10,000 x g for 10 min at 4□. An aliquot of the supernatant was then used for RNA purification with on-column DNase-I treatment (Direct-Zol RNA Microprep R2060, Zymo Research). RNA concentration and purity was determined by spectrophotometry (NanoDrop 1000, Thermo Fisher Scientific) while RNA fragment size distribution was assessed by gel electrophoresis (Tapestation HS-RNA, Agilent Technologies).

Reverse transcription and quantitative PCR (RT-qPCR)

Equal volumes of isolated RNA from the RNase-treated mitochondria samples (to account for differences in total RNA yield between samples due to RNase treatment) were reverse transcribed to first-strand cDNA in a 20 µL reaction along with no-template and no-RTase controls (Applied Biosystems High Capacity RT kit #4368814). Quantitative PCR was performed in triplicate (Agilent AriaMX G8830A) on 4 ng of cDNA in a 10 µL reaction consisting of SYBR green master mix (Applied Biosystems #4367659) with 0.3 µM forward and reverse primers (Table 1).

Table 1. List of RT qPCR primers

Target	**Forward (5' -3')**	**Reverse (5' -3')**	**Accession ID**
Mt-co3	GACGGAATTTACGGCTCAACAT	AATTAGGAAAGTTGAGCCAATAATTACG	>NC_001665.2 Rattus norvegicus strain BN/SsNHsdMCW mitochondrion, complete genome

Cox4i1	GTGCTGATCTGGGAGAAGAGCTA	GGTTGACCTTCATGTCCAGCAT	>NM_017202.1 Rattus norvegicus cytochrome c oxidase subunit 4i1 (Cox4i1), mRNA; nuclear gene for mitochondrial product
eGFP	ACTTCTTCAAGTCCGCCATG	AGCTCGATGCGGTTCACCAG	>XM_013480425.1 Eimeria maxima Green fluorescent protein, related partial mRNA

Thermal conditions used for qPCR were 10 min at 95□ (activation) then 40 cycles of 15 s at 95°C (denature) and 60 s at 55-60□ (anneal/extend). A dissociation curve was performed to confirm the amplification of a single product. Quantification cycle (C_q) thresholds were calculated using software (Agilent Aria v1.5) expressed after linear transformation.

Myoblast small RNA sequencing and bioinformatics

Total RNA isolated from individual (n=7) L6 mitochondria samples was pooled into a single tube, from which serial dilutions ranging from 0.3-20 ng/µL were prepared. Complementary DNA libraries were then prepared using a range of mitochondrial RNA inputs (final input range 1.8-120 ng) using the NEBNext Multiplex Small RNA Library Prep Set (New England Biolabs.). To investigate the efficiency of small RNA library preparation across a range of mitochondrial RNA inputs, libraries were prepared either according to the manufacturer's recommendations for low RNA inputs (NEBNext 3´ and 5' SR Adaptors, and RT primer for Ilumina diluted 0.5X, 15 PCR cycles) or with modifications (NEBNext 3´ and 5' SR Adaptors, and RT primer for Ilumina diluted 0.3X or 0.1X, 20 PCR cycles). cDNA concentration was determined by fluorometric quantitation (Qubit 1xdsDNA, Thermo Fisher Scientific) while cDNA fragment size distribution was assessed by gel electrophoresis (Tapestation HS-D1000, Agilent Technologies).

An equimolar pool of all uniquely indexed small RNA libraries was prepared. Twenty-five µL of the equimolar pool was loaded across two lanes on a 6% Novex TBE polyacrylamide gel (Thermo Fischer Scientific), with 5 µL Quick-Load pBR322 DNA-MspI Molecular Marker (New England Biolabs Inc.) in a separate lane. The buffer dam was filled with 600 mL 1X TBE running buffer and the gel run at 120V for 1h. The gel was then incubated with 50 mL 1X TBE spiked with 1X SYBR Gold Nucleic Acid Gel Stain (Thermo Fischer Scientific), before being visualised on a Safe Imager 2.0 Blue-Light Transilluminator (Invitrogen) following exposure to UV-Blue (470 nm) light. Fragments corresponding to the 130-160 bp region were manually excised, before suspended and then crushed in 250 µL gel elution buffer (New England Biolabs Inc.). To increase the recovery of low concentrations of small nucleic acids, cDNA was precipitated overnight at -20°C with 0.3 M sodium acetate (pH 5.5), 4X volumes of 100% ethanol and 1 µL linear acrylamide carrier. Following

overnight precipitation, the solution was centrifuged at 16,000x*g* for 60 minutes to pellet the cDNA fragment. The cDNA pellet was washed twice with 80% ethanol and resuspend in 12 µL TE buffer. Fragment size distribution of the gel-extracted cDNA pool was assessed by gel electrophoresis (Tapestation HS-D1000, Agilent Technologies).

RNA sequencing was performed by the Deakin University Genomics Core on the Illumina MiniSeq platform. A 1.3 pM loading pool was prepared with 20% Phi-X spike-in and was sequenced on a single-end 75 bp run. Sequenced reads underwent quality checks with FastQC before the adapter and reads <20nt were trimmed. Small RNAs, including miRNAs, are not well sequenced in the rat genome but are conserved between rat and mouse species. Reads were mapped to known mature mouse miRNAs accessible from miRbase v22.0. Raw read counts were normalised by the size of each individual library. Counts were visualised using GraphPad Prism (v7).

Rodent study ethical approval and procedures

All experimental procedures were approved by the Deakin University Animal Ethics Committee (G02-2019). All animals were housed and treated in accordance with standards set by Deakin University's Animal Welfare Committee, which complies with the ethical and governing principles outlined in the Australian code for the care and use of animals for scientific purposes. Wistar Kyoto male rats were obtained from the Animal Resource Centre, Perth, Western Australia. Rats were housed in pairs and maintained with a 12-hour light/dark cycle, constant temperature of 21 ± 2°C, and humidity levels between 40 and 70%. Rats had *ad libitum* access to standard chow diet and tap water. At 9-weeks of age, animals were humanely killed following dissection of the heart under heavy anaesthesia using 5% isoflurane gas. The gastrocnemius muscle was rapidly excised then the inner red portion was dissected. A portion of this was snap frozen in liquid nitrogen for subsequent whole muscle RNA analyses, and a separate ~ 100 mg piece was taken for mitochondrial isolation. This was immediately placed in 1 mL ice-cold lysis buffer and minced using fine scissors before mechanical homogenisation with an ice-cold Teflon-tipped glass dounce homogeniser (10 passes with rotation at 350 rpm). Intact mitochondria were then isolated using the magnetic-bead immunoprecipitation method as described above for L6 myoblasts except with the following RNase treatment conditions: RNase-A 340 µg/mL in a reaction with ~20 µg total mitochondrial protein performed for 1 hour at 37□, after which 5 µL proteinase-K (stock concentration 600 mAU/mL) was then added to inactivate RNase activity (Barrey et al., 2011). Each tube was briefly inverted before the mitochondria solutions were then centrifuged at 8000 x g for 10 min at 4□. The supernatant was aspirated and the pellet was washed twice with 100 µL ice-cold storage buffer. The RNase-treated mitochondrial pellet was resuspended in 100 uL storage buffer then frozen at -80□ until RNA extraction.

RNA extraction from rat muscle tissue and isolated mitochondria

For RNA extraction from whole red gastrocnemius muscle, ~15 mg frozen tissue was placed in a liquid nitrogen pre-chilled cyrotube with a 5 mm stainless steel bead. The tissue was then mechanically disrupted (2 cycles at 4m/s for 10 s, MP Biomedical FastPrep). Tri-reagent (600 uL) was added, then RNA extracted (Zymo DirectZol RNA Miniprep #R2050). For RNA extraction from isolated mitochondria from the respective red portion of gastrocnemius muscle, frozen samples were thawed in the presence of 5 volumes of TRI-reagent (Qiagen), pipette mixed thoroughly then centrifuged at 16,000 x g for 1 min. RNA extraction was then performed with on-column DNase I treatment (Zymo Research DirectZol RNA Mircroprep #2060). Extracted RNA was tested for purity on Nanodrop, concentration with Qubit HS RNA assay (Thermo Fisher) then RNA integrity number (RIN) was determined using a Tapestation (Agilent) with High Sensitivity RNA reagents. All RINs from whole tissue RNA were ≥7.0.

Rat muscle tissue and isolated mitochondria total RNA sequencing

Total RNA from whole-tissue (50 ng) and isolated mitochondria (10 ng) were converted to cDNA libraries (Zymo-Seq RiboFree Total RNA #R300, Zymo Research). Briefly, ribosomal RNA was depleted, then remaining transcripts were fragmented and converted to cDNA using random priming. After second strand synthesis, the ends of the cDNA were enzymatically repaired and Illumina-compatible sequencing adaptors were ligated. Library size (TapeStation, Agilent) and concentration (Qubit) was assessed prior to sequencing. RNA sequencing was performed by the Deakin University Genomics Core on the Illumina NovaSeq 6000 platform. Reads underwent adapter trimming and quality check with Skewer then mapped to the rat genome (Ensembl version 99) with STAR aligner v2.7.2a. STAR generated read counts were collated in R version 4.0.3 (R Development Core Team, 2010). Normalised counts were visualised using GraphPad Prism (v7). Analysis of differential expression was performed using Voom/Limma in Degust v 4.1.5 (Powell, 2019). Transcripts with a false discovery rate (FDR) <0.05 were considered differentially expressed.

Statistical analysis

Small RNA-seq data was analysed by paired t-test. RNase-A dose-response data were tested for normality of variance and then analysed by one- or two-way ANOVA with Tukey's post hoc test for multiple comparisons using GraphPad Prism (v7). All data are presented as mean (SD) with significance accepted at $p<0.05$.

Acknowledgments

We acknowledge Gisella Mazzarino and Amandi Gunawardena for their assistance with animal experiments and tissue collection. We acknowledge Sarah Alexander for her assistance with female participant recruitment. Severine Lamon is supported by an Australian Research Council Future Fellowship (FT10100278).

Author contributions

Conceptualization: JLS, AJT, SN, S.Lamon, GDW

Conducted experiments: JLS, AJT, GDW, S.Loke

Conducted human studies: JLS, GDW, S.Lamon, HD

Data analysis (bioinformatics): MZ, LC

Data analysis and visualisation: JLS, AJT

Manuscript – original draft: JLS & AJT

Manuscript– review and editing: all authors.

Approved final version of manuscript: all authors.

REFERENCES

ABDELMOEZ, A. M., SARDÓN PUIG, L., SMITH, J. A. B., GABRIEL, B. M., SAVIKJ, M., DOLLET, L., CHIBALIN, A. V., KROOK, A., ZIERATH, J. R. & PILLON, N. J. 2020. Comparative profiling of skeletal muscle models reveals heterogeneity of transcriptome and metabolism. *Am J Physiol Cell Physiol,* 318**,** C615-c626.

BANDIERA, S., RUBERG, S., GIRARD, M., CAGNARD, N., HANEIN, S., CHRETIEN, D., MUNNICH, A., LYONNET, S. & HENRION-CAUDE, A. 2011. Nuclear outsourcing of RNA interference components to human mitochondria. *PLoS One,* 6**,** e20746.

BARREY, E., SAINT-AURET, G., BONNAMY, B., DAMAS, D., BOYER, O. & GIDROL, X. 2011. Pre-microRNA and mature microRNA in human mitochondria. *PLoS One,* 6**,** e20220.

DAS, S., FERLITO, M., KENT, O. A., FOX-TALBOT, K., WANG, R., LIU, D., RAGHAVACHARI, N., YANG, Y., WHEELAN, S. J., MURPHY, E. & STEENBERGEN, C. 2012. Nuclear miRNA regulates the mitochondrial genome in the heart. *Circ Res,* 110**,** 1596-603.

DASGUPTA, N., PENG, Y., TAN, Z., CIRAOLO, G., WANG, D. & LI, R. 2015. miRNAs in mtDNA-less cell mitochondria. *Cell Death Discov,* 1**,** 15004.

GAO, F., CAI, Y., KAPRANOV, P. & XU, D. 2020. Reverse-genetics studies of lncRNAs—what we have learnt and paths forward. *Genome Biology,* 21**,** 93.

GOLD, V. A., CHROSCICKI, P., BRAGOSZEWSKI, P. & CHACINSKA, A. 2017. Visualization of cytosolic ribosomes on the surface of mitochondria by electron cryo-tomography. *EMBO Rep,* 18**,** 1786-1800.

JAGANNATHAN, R., THAPA, D., NICHOLS, C. E., SHEPHERD, D. L., STRICKER, J. C., CROSTON, T. L., BASELER, W. A., LEWIS, S. E., MARTINEZ, I. & HOLLANDER, J. M. 2015. Translational Regulation of the Mitochondrial Genome Following Redistribution of Mitochondrial MicroRNA (MitomiR) in the Diabetic Heart. *Circulation. Cardiovascular genetics,* 8**,** 785-802.

LONG, Y., WANG, X., YOUMANS, D. T. & CECH, T. R. 2017. How do lncRNAs regulate transcription? *Science Adv,* 3**,** eaao2110.

LUNG, B., ZEMANN, A., MADEJ, M. J., SCHUELKE, M., TECHRITZ, S., RUF, S., BOCK, R. & HUTTENHOFER, A. 2006. Identification of small non-coding RNAs from mitochondria and chloroplasts. *Nucleic Acids Res,* 34**,** 3842-52.

MERCER, T. R., NEPH, S., DINGER, M. E., CRAWFORD, J., SMITH, M. A., SHEARWOOD, A. M., HAUGEN, E., BRACKEN, C. P., RACKHAM, O., STAMATOYANNOPOULOS, J. A., FILIPOVSKA, A. & MATTICK, J. S. 2011. The human mitochondrial transcriptome. *Cell,* 146**,** 645-58.

NIE, Y., SATO, Y., WANG, C., YUE, F., KUANG, S. & GAVIN, T. P. 2016. Impaired exercise tolerance, mitochondrial biogenesis, and muscle fiber maintenance in miR-133a-deficient mice. *Faseb j,* 30**,** 3745-3758.

NIELSEN, S., SCHEELE, C., YFANTI, C., AKERSTROM, T., NIELSEN, A. R., PEDERSEN, B. K. & LAYE, M. J. 2010. Muscle specific microRNAs are regulated by endurance exercise in human skeletal muscle. *J Physiol,* 588**,** 4029-37.

NOH, J. H., KIM, K. M., ABDELMOHSEN, K., YOON, J.-H., PANDA, A. C., MUNK, R., KIM, J., CURTIS, J., MOAD, C. A. & WOHLER, C. M. 2016. HuR and GRSF1 modulate the nuclear export and mitochondrial localization of the lncRNA RMRP. *Genes Dev,* 30**,** 1224-1239.

POWELL, D. 2019. Degust v4.1.1. Zenodo. doi.org/10.5281/zenodo.3501067.

RAJKUMAR, A. P., QVIST, P., LAZARUS, R., LESCAI, F., JU, J., NYEGAARD, M., MORS, O., BØRGLUM, A. D., LI, Q. & CHRISTENSEN, J. H. 2015. Experimental validation of methods for differential gene expression analysis and sample pooling in RNA-seq. *BMC Genomics,* 16**,** 548.

RUSSELL, A. P., FOLETTA, V. C., SNOW, R. J. & WADLEY, G. D. 2014. Skeletal muscle mitochondria: a major player in exercise, health and disease. *Biochim Biophys Acta,* 1840**,** 1276-84.

504 RUSSELL, A. P., LAMON, S., BOON, H., WADA, S., GULLER, I., BROWN, E. L., CHIBALIN, A. V., ZIERATH,
505 J. R., SNOW, R. J., STEPTO, N., WADLEY, G. D. & AKIMOTO, T. 2013. Regulation of miRNAs in
506 human skeletal muscle following acute endurance exercise and short-term endurance
507 training. *J Physiol,* 591**,** 4637-53.
508 SHORE, S., HENDERSON, J. M., LEBEDEV, A., SALCEDO, M. P., ZON, G., MCCAFFREY, A. P., PAUL, N. &
509 HOGREFE, R. I. 2016. Small RNA Library Preparation Method for Next-Generation Sequencing
510 Using Chemical Modifications to Prevent Adapter Dimer Formation. *PLoS One,* 11**,** e0167009.
511 SILVER, J., WADLEY, G. & LAMON, S. 2018. Mitochondrial regulation in skeletal muscle: A role for
512 non-coding RNAs? *Experimental Physiology* 103**,** 1132-1144.
513 SPINELLI, J. B. & HAIGIS, M. C. 2018. The multifaceted contributions of mitochondria to cellular
514 metabolism. *Nat Cell Biol,* 20**,** 745-754.
515 SRIPADA, L., TOMAR, D., PRAJAPATI, P., SINGH, R., SINGH, A. K. & SINGH, R. 2012. Systematic
516 Analysis of Small RNAs Associated with Human Mitochondria by Deep Sequencing: Detailed
517 Analysis of Mitochondrial Associated miRNA. *PLoS ONE,* 7**,** e44873.
518 TAKELE ASSEFA, A., VANDESOMPELE, J. & THAS, O. 2020. On the utility of RNA sample pooling to
519 optimize cost and statistical power in RNA sequencing experiments. *BMC Genomics,* 21**,** 312.
520 WADLEY, G. D., LAMON, S., ALEXANDER, S. E., MCMULLEN, J. R. & BERNARDO, B. C. 2019. Non-
521 coding RNAs regulating cardiac muscle mass. *Journal of Applied Physiology,* 127**,** 633-644.
522 WANG, G., CHEN, H. W., OKTAY, Y., ZHANG, J., ALLEN, E. L., SMITH, G. M., FAN, K. C., HONG, J. S.,
523 FRENCH, S. W., MCCAFFERY, J. M., LIGHTOWLERS, R. N., MORSE, H. C., 3RD, KOEHLER, C. M.
524 & TEITELL, M. A. 2010. PNPASE regulates RNA import into mitochondria. *Cell,* 142**,** 456-67.
525 WANG, X., SONG, C., ZHOU, X., HAN, X., LI, J., WANG, Z., SHANG, H., LIU, Y. & CAO, H. 2017.
526 Mitochondria Associated MicroRNA Expression Profiling of Heart Failure. *Biomed Res Int,*
527 2017**,** 4042509.
528 WITZEL, H. 1963. The Function of the Pyrimidine Base in the Ribonuclease Reaction. *In:* DAVIDSON, J.
529 N. & COHN, W. E. (eds.) *Progress in Nucleic Acid Research and Molecular Biology.* Academic
530 Press.
531 ZHANG, X., ZUO, X., YANG, B., LI, Z., XUE, Y., ZHOU, Y., HUANG, J., ZHAO, X., ZHOU, J., YAN, Y.,
532 ZHANG, H., GUO, P., SUN, H., GUO, L., ZHANG, Y. & FU, X. D. 2014. MicroRNA directly
533 enhances mitochondrial translation during muscle differentiation. *Cell,* 158**,** 607-19.
534 ZURLO, F., LARSON, K., BOGARDUS, C. & RAVUSSIN, E. 1990. Skeletal muscle metabolism is a major
535 determinant of resting energy expenditure. *J Clin Invest,* 86**,** 1423-7.

536

537

538

FIGURE LEGENDS

Figure 1. Overview of TOMM22 immunoprecipitation based method for mitochondrial isolation

Figure 2. Protease treatment of mitochondria isolated from L6 myocytes. Isolated mitochondria were incubated with or without proteinase-K (20 µg/mL) and detergent (1% triton-X). Marker proteins of subcellular compartments were then probed by immunoblot. Blots are representative of *n*=2 technical replicates from a single mitochondrial isolation preparation.

Figure 3. RNase-A treatment of mitochondria isolated from L6 myocytes. Isolated mitochondria were incubated with or without RNase-A (1-1000 µg/mL) in the presence or absence of detergent (1% triton-X). The levels of representative mtDNA (*Mtco3*) and nuclear (*Cox4i1*) encoded genes were then assessed by RT-qPCR in addition to an exogenous mRNA spike-in control (*eGFP*) added to isolated mitochondria (but not to the whole cell lysate). Data are mean(SD) for *N*=3 technical replicates from a single mitochondrial isolation preparation.

Figure 4. Small RNA-seq library preparation from mitochondrial RNA. Representative electropherogram traces of libraries generated with the standard 0.5X dilution of 3' and 5' adapters produces large amounts of adapter-dimer (red box) and does not ligate to mitochondria miRNAs with either A) 120 ng or B) 60 ng mitochondrial RNA input. Lower molar ratios (0.3X dilution) of 3' and 5' adapters produces the target miRNA library (green box) with C) 60ng and D) 1.8ng mitochondria RNA. Peaks at 25 and 1500 bp are internal size standards.

Figure 5. Small RNA-Seq on isolated mitochondria from L6 myocytes. Small RNA libraries were prepared from 1.8 to 60 ng mitochondria RNA with modified-0.3X (n=6) or modified-0.1X (n=4) protocols. The total number of reads (p=0.79) and total mapped miRNA reads (p=0.19) were not different between protocols. Student's paired t-test, *n*=1 at each RNA input.

Figure 6. Neither mitochondrial RNA input nor library preparation protocols limit the number of mature miRNAs that can be detected from mitochondrial RNA. A) The number of mature miRNA species detected across all mitochondria RNA inputs was not different (p=0.60, student's paired t-test) following modified-0.3X (m-0.3X; n=6) and modified-0.1X (m-0.1X; n=4) protocols. Each point represents an independent library prepared from 1.8-60ng mitochondrial RNA.

Figure 7. The relative abundance of miRNAs within each sample is comparable between small RNA libraries prepared from high, moderate and low mitochondrial RNA inputs. Venn diagrams depicting unique and shared miRNAs detected from 60ng mitochondria RNA when compared to **A)** 1.8ng, **B)** 7.5ng and **C)** 30ng mitochondria RNA, prepared using the modified-0.3X library preparation approach. The relative distribution of miRNAs detected at each RNA input was expressed relative to mmu-miR-let-7c-2. Differences in the relative distribution of miRNAs between the highest RNA input and serial RNA dilutions (**D)** 1.8ng, **E)** 7.5ng and **F)** 30ng) are depicted by grey dots (<5-fold change when compared to 60ng), red dots (>5-fold change when compared to 60ng) and green dots (>10-fold change when compared to 60ng). Highly abundant miRNAs across all RNA inputs (including the let-7 family and mmu-miR-206) are shown in orange dots.

Figure 8. RNase-treated mitochondria isolated from rat skeletal muscle tissue contains nuclear-encoded non-coding RNAs. Whole-transcriptome RNA sequencing of isolated mitochondria and respective whole muscle tissue (rat gastrocnemius) shows that the isolated mitochondria were free of **A)** muscle sarcomere related mRNAs **B)** and nuclear-encoded mRNAs involved in the mitochondrial electron transport chain, while **C)** mtDNA encoded mitochondrial electron transport chain genes were present. **D)** Scatterplot depicting the abundance of RNA classes in isolated mitochondria relative to whole muscle; each point represents the mean normalised abundance (reads per million, RPM) of an individual gene from n=6 biological replicates.

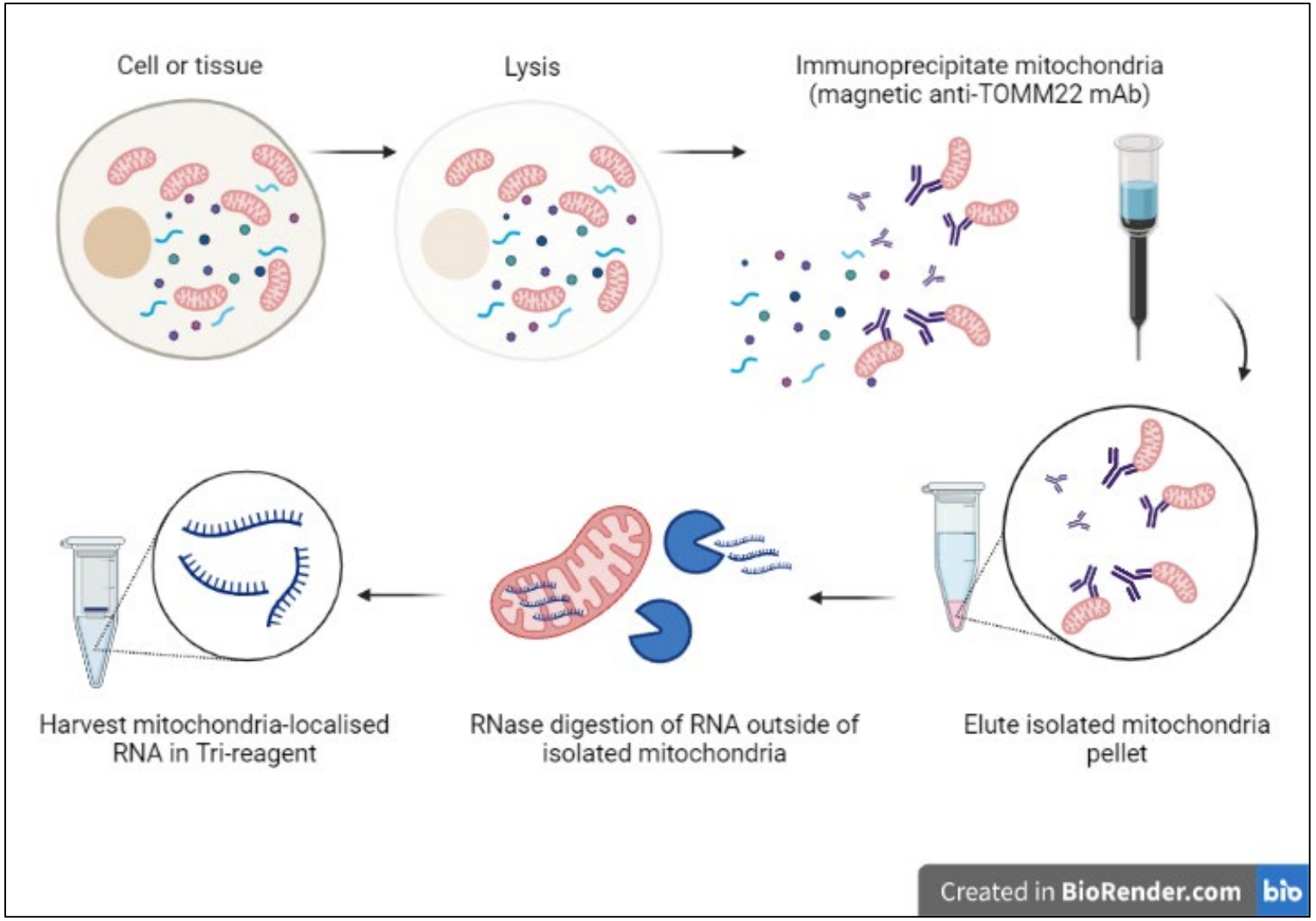
Cell or tissue
Lysis
Immunoprecipitate mitochondria
(magnetic anti-TOMM22 mAb)
Harvest mitochondria-localised
RNA in Tri-reagent
RNase digestion of RNA outside of
isolated mitochondria
Elute isolated mitochondria
pellet
Created in BioRender.com
bio

Figure 1.

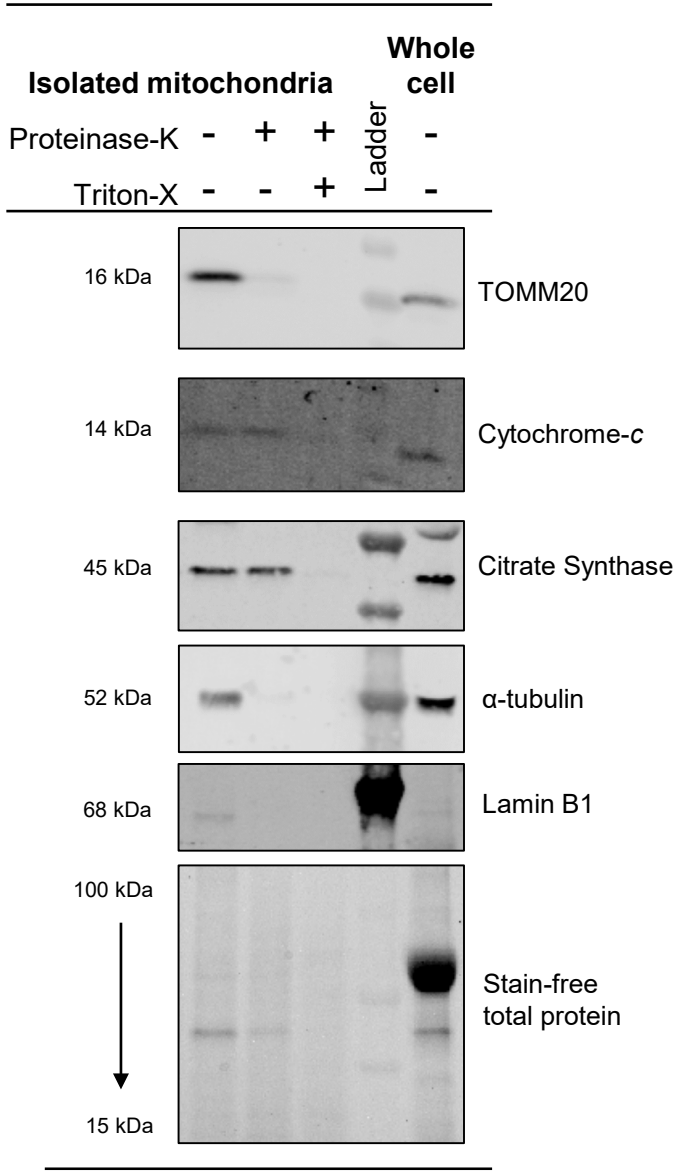
Isolated mitochondria
Whole cell
Proteinase-K - + + - -
Triton-X - - + - -
Ladder
16 kDa
TOMM20
14 kDa
Cytochrome-c
45 kDa
Citrate Synthase
52 kDa
α-tubulin
68 kDa
Lamin B1
100 kDa
15 kDa
Stain-free
total protein

Figure 2.

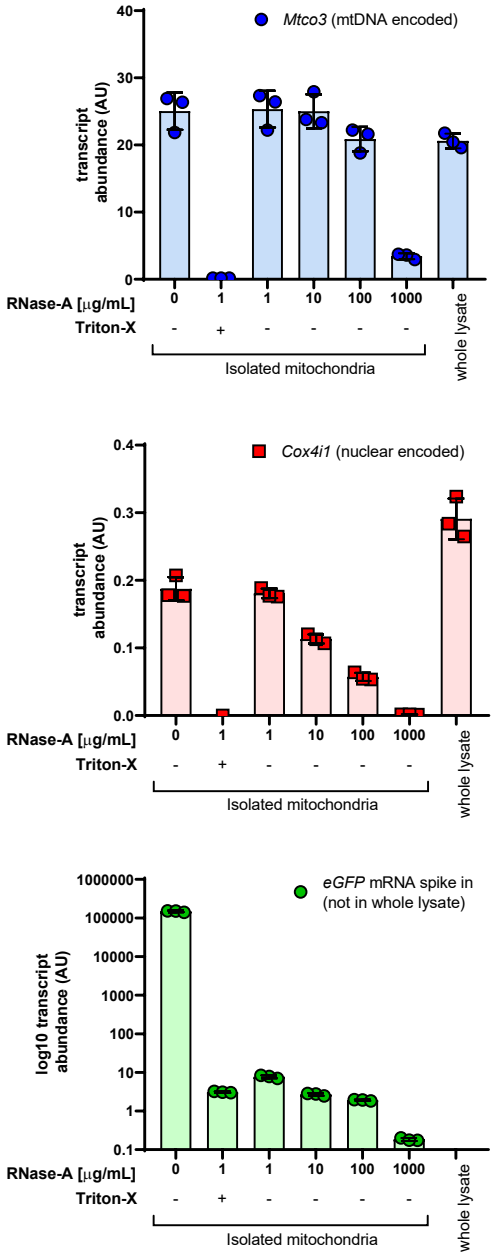
Mtco3 (mtDNA encoded)
transcript abundance (AU)
40
30
20
10
0
RNase-A [μg/mL]
0
1
1
10
100
1000
Triton-X
-
+
-
-
-
-
Isolated mitochondria
whole lysate
Cox4i1 (nuclear encoded)
transcript abundance (AU)
0.4
0.3
0.2
0.1
0.0
RNase-A [μg/mL]
0
1
1
10
100
1000
Triton-X
-
+
-
-
-
-
Isolated mitochondria
whole lysate
eGFP mRNA spike in
(not in whole lysate)
log10 transcript abundance (AU)
1000000
100000
10000
1000
100
10
1
0.1
RNase-A [μg/mL]
0
1
1
10
100
1000
Triton-X
-
+
-
-
-
-
Isolated mitochondria
whole lysate

Figure 3.

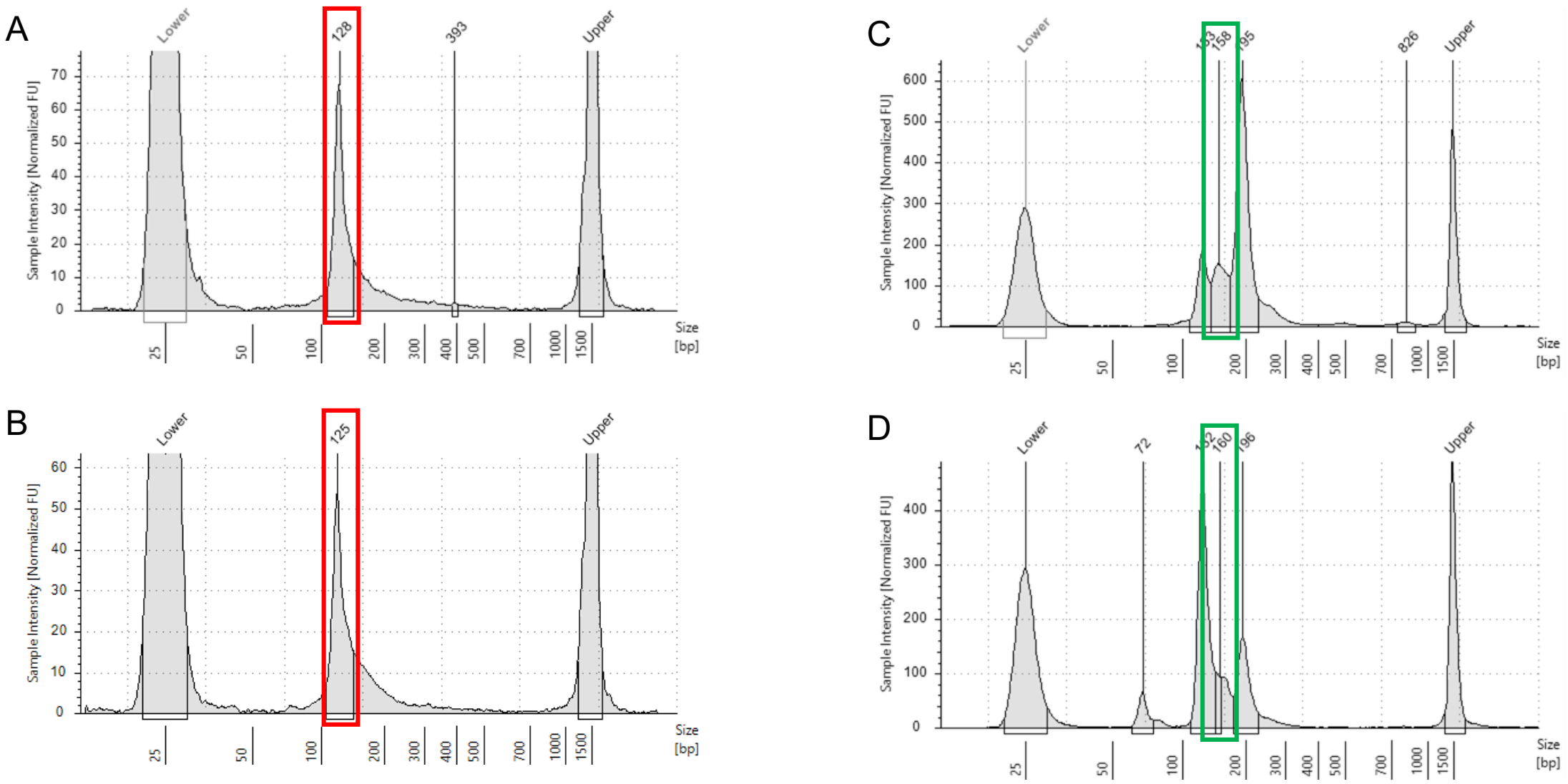
A
Lower
128
393
Upper
Sample Intensity [Normalized FU]
Size [bp]
B
Lower
125
Upper
Sample Intensity [Normalized FU]
Size [bp]
C
Lower
158
195
826
Upper
Sample Intensity [Normalized FU]
Size [bp]
D
Lower
72
160
196
Upper
Sample Intensity [Normalized FU]
Size [bp]

Figure 4.

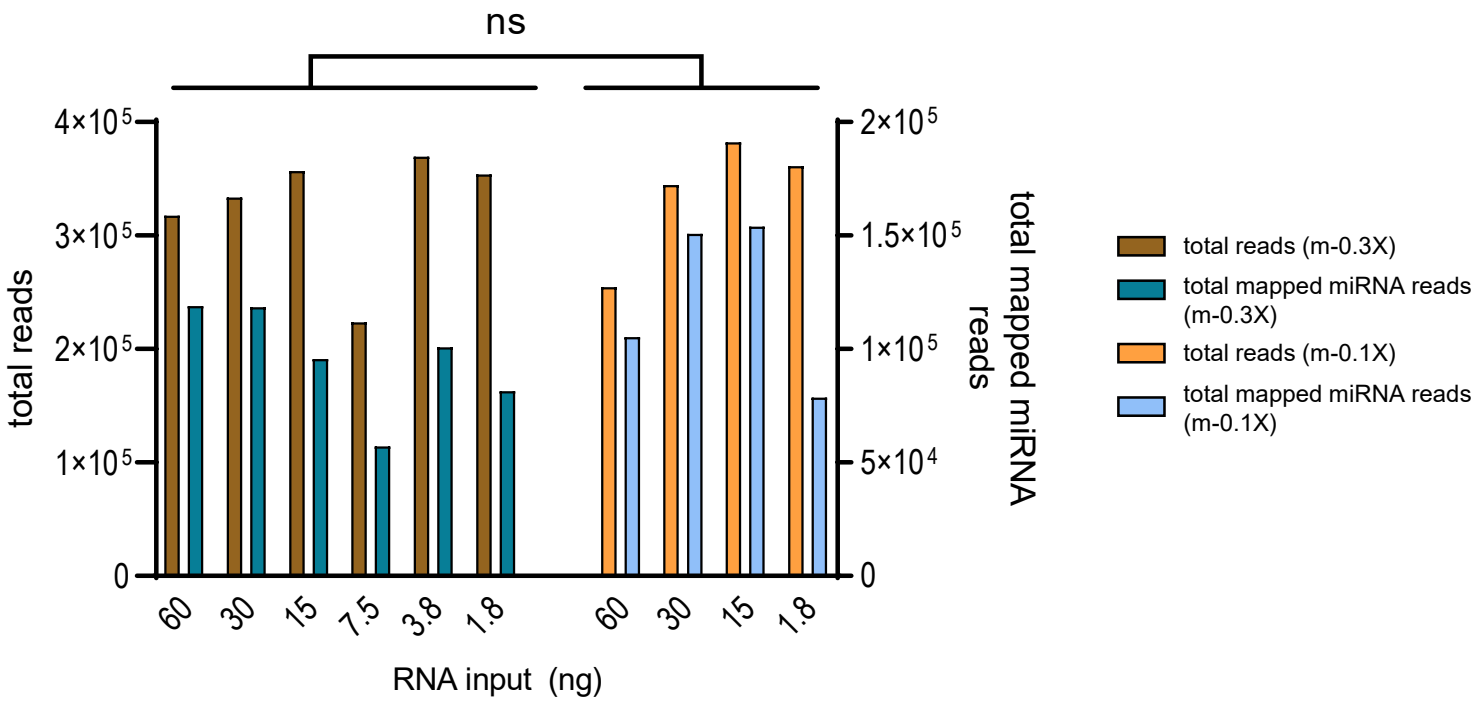
ns
4×10^5
3×10^5
2×10^5
1×10^5
0
total reads
2×10^5
1.5×10^5
1×10^5
5×10^4
0
total mapped miRNA reads
60
30
15
7.5
3.8
1.8
60
30
15
1.8
RNA input (ng)
total reads (m-0.3X)
total mapped miRNA reads (m-0.3X)
total reads (m-0.1X)
total mapped miRNA reads (m-0.1X)

Figure 5.

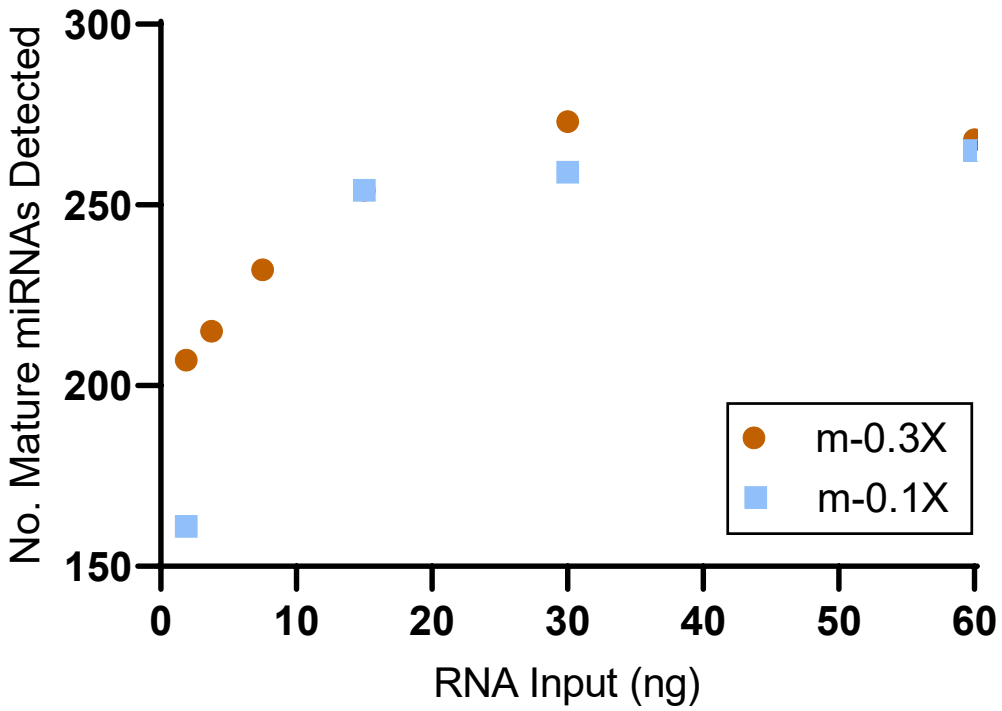
300
250
200
150
No. Mature miRNAs Detected
0
10
20
30
40
50
60
RNA Input (ng)
m-0.3X
m-0.1X

Figure 6.

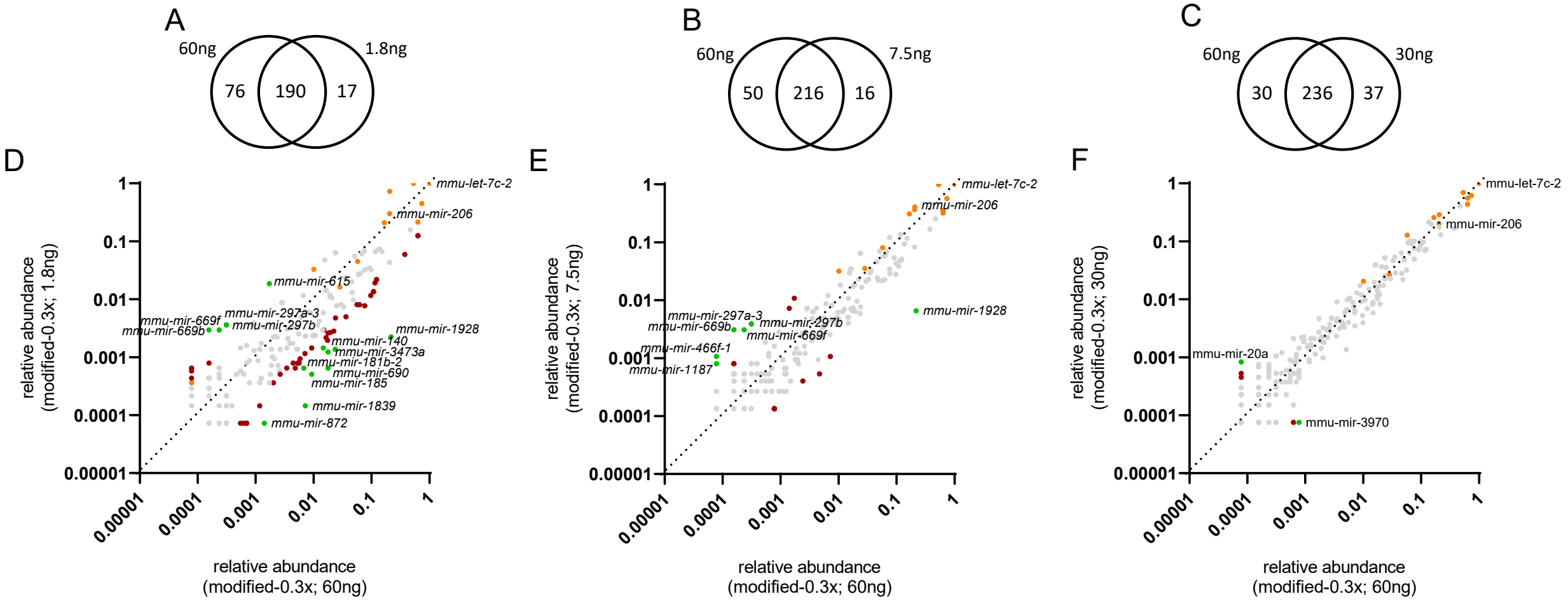
A
60ng
1.8ng
76
190
17
B
60ng
7.5ng
50
216
16
C
60ng
30ng
30
236
37
D
E
F
relative abundance
(modified-0.3x; 1.8ng)
relative abundance
(modified-0.3x; 7.5ng)
relative abundance
(modified-0.3x; 30ng)
relative abundance
(modified-0.3x; 60ng)
1
0.1
0.01
0.001
0.0001
0.00001
mmu-let-7c-2
mmu-mir-206
mmu-mir-615
mmu-mir-669f
mmu-mir-669b
mmu-mir-297a-3
mmu-mir-297b
mmu-mir-1928
mmu-mir-140
mmu-mir-3473a
mmu-mir-181b-2
mmu-mir-690
mmu-mir-185
mmu-mir-1839
mmu-mir-872
mmu-mir-466f-1
mmu-mir-1187
mmu-mir-20a
mmu-mir-3970

Figure 7.

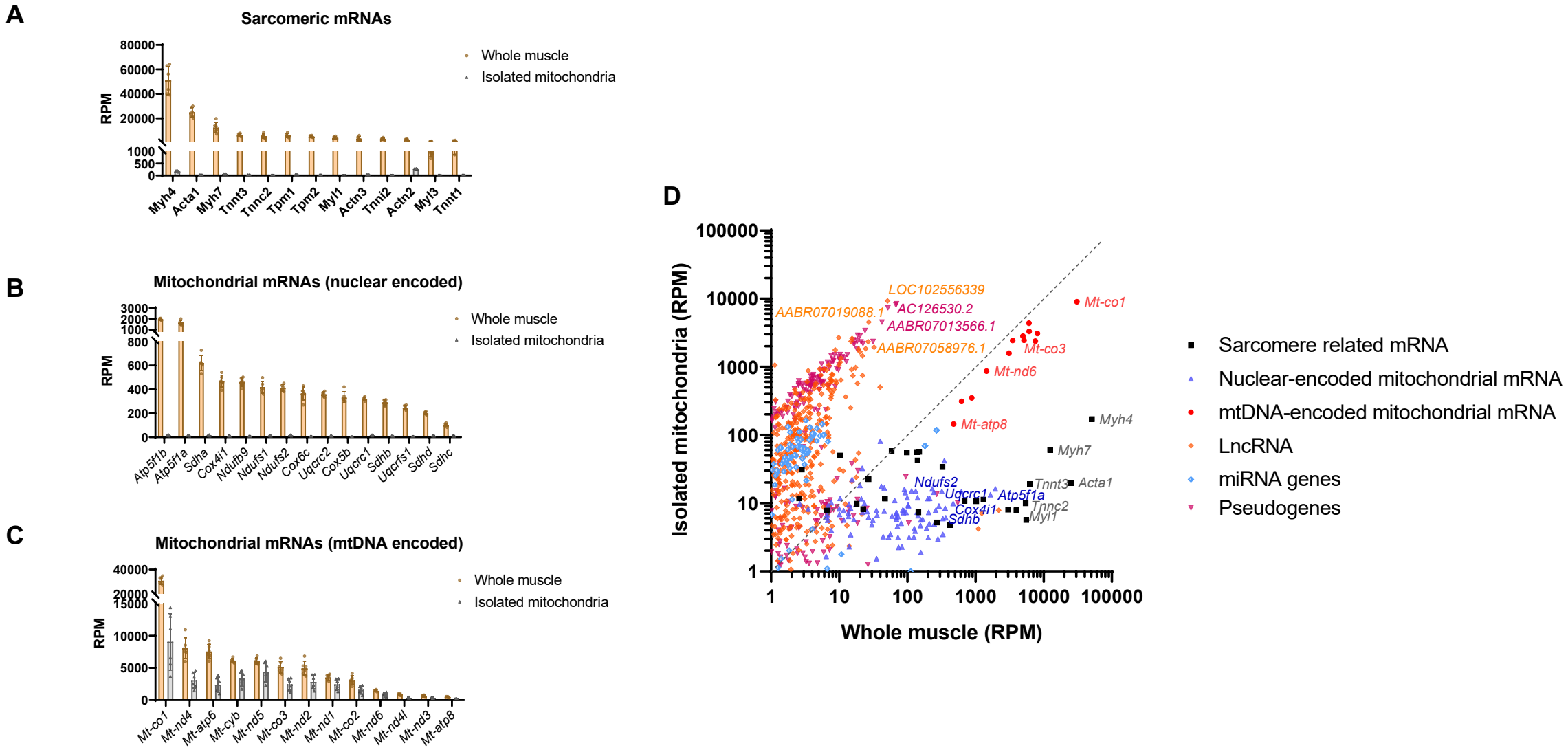
A
Sarcomeric mRNAs
RPM
Whole muscle
Isolated mitochondria
Myh4
Acta1
Myh7
Tnnt3
Tnnc2
Tpm1
Tpm2
Myl1
Actn3
Tnni2
Actn2
Myl3
Tnnt1
B
Mitochondrial mRNAs (nuclear encoded)
Atp5f1b
Atp5f1a
Sdha
Cox4i1
Ndufb9
Ndufs1
Ndufs2
Cox6c
Uqcrc2
Cox5b
Uqcrc1
Sdhb
Uqcrfs1
Sdhd
Sdhc
C
Mitochondrial mRNAs (mtDNA encoded)
Mt-co1
Mt-nd4
Mt-atp6
Mt-cyb
Mt-nd5
Mt-co3
Mt-nd2
Mt-nd1
Mt-co2
Mt-nd6
Mt-nd4l
Mt-nd3
Mt-atp8
D
Isolated mitochondria (RPM)
Whole muscle (RPM)
LOC102556339
AC126530.2
AABR07019088.1
AABR07013566.1
AABR07058976.1
Mt-co1
Mt-co3
Mt-nd6
Mt-atp8
Myh4
Myh7
Tnnt3
Acta1
Tnnc2
Myl1
Ndufs2
Uqcrc1
Atp5f1a
Cox4i1
Sdhb
Sarcomere related mRNA
Nuclear-encoded mitochondrial mRNA
mtDNA-encoded mitochondrial mRNA
LncRNA
miRNA genes
Pseudogenes

Figure 8.